Shape Anisotropy: Tensor Distance to Anisotropy Measure

Yonas T. Weldeselassie, Saba El-Hilo and M. Stella Atkins

Medical Image Analysis Lab, School of Computing Science, Simon Fraser University

ABSTRACT

Fractional anisotropy (FA), defined as the distance of a diffusion tensor from its closest isotropic tensor, has been extensively studied as quantitative anisotropy measure for diffusion tensor magnetic resonance images (DT-MRI). It has been used to reveal the white matter profile of brain images, as guiding feature for seeding and stopping in fiber tractography and for the diagnosis and assessment of degenerative brain diseases. Despite its extensive use in DT-MRI community, however, not much attention has been given to the mathematical correctness of its derivation from diffusion tensors which is achieved using Euclidean dot product in **9D** space. But, recent progress in DT-MRI have shown that the space of diffusion tensors does not form a Euclidean vector space and thus Euclidean dot product is not appropriate for tensors. In this paper, we propose a novel and robust rotationally invariant diffusion anisotropy measure derived using the recently proposed Log-Euclidean and J-divergence tensor distance measures. An interesting finding of our work is that given a diffusion tensor, its closest isotropic tensor is different for different tensor distance used. We demonstrate qualitatively that our new anisotropy measure reveals superior white matter profile of DT-MR brain images and analytically show that it has a higher signal to noise ratio than FA.

Keywords: Diffusion tensor magnetic resonance imaging, tensor distance, fractional anisotropy, shape anisotropy

1. INTRODUCTION

Diffusion tensor magnetic resonance imaging (DT-MRI) is a non-invasive imaging technique that measures the self-diffusion of water molecules in the body; thus capturing the microstructure of the underlying tissues. It results in a 3D image where at each voxel the direction of water diffusion is locally modeled by a Gaussian probability density function whose covariance matrix is a second order 3×3 symmetric positive definite matrix (diffusion tensor).

Measurement of diffusion tensors on a voxel-by-voxel basis has lead to the development of scalar quantities, called indices of anisotropy, that resemble histological or physiological stains characterizing the intrinsic features of tissue microstructure and microdynamics. The most commonly used such scalar diffusion anisotropy measure is fractional anisotropy (FA),[1] which is defined as the distance of a tensor from its closest isotropic tensor. It is rotationally invariant and, therefore, objective and insensitive to the choice of laboratory coordinate system. It has been widely used for revealing the white matter in brain images, as a parameter for seeding and stopping in fiber tractography, and for the diagnosis and assessment of degenerative brain diseases such as multiple sclerosis, Parkinson's disease, schizophrenia, and Alzheimer's disease and classification of patients and healthy subjects in clinical settings.[2–6]

Despite the extensive use of FA in DT-MRI community, however, not much attention has been given to the mathematical correctness of its derivation from diffusion tensors, which is achieved using generalized tensor dot product in **9D** Euclidean space;[1] yet recent progress in DT-MRI research have shown that the space of diffusion tensors does not form a Euclidean vector space and thus Euclidean norm is not appropriate for tensors. To this end, new appropriate tensor distance measures that take into account the manifold of the space of diffusion tensors have been proposed. These distance measures include the J-divergence,[7] Log-Euclidean[8] and Riemannian distance metric.[9,10] Therefore it is more consistent with the definition of FA to use these appropriate tensor distance measures instead of Euclidean tensor dot products in deriving anisotropy measures for diffusion tensors.

Send correspondence to Yonas T. Weldeselassie (E-mail: yonas@cs.sfu.ca, Telephone: 1 778 782 5509)

In this paper, we propose a novel and robust diffusion anisotropy measure that is rotationally invariant and scale invariant derived using the J-divergence and Log-Euclidean distance measures. The proposed anisotropy measure is computed by first decomposing the tensor distance metrics to shape and orientation distance components[11] and then use the shape distance component for measuring distance of a diffusion tensor from its closest isotropy. An interesting consequence of applying different distance measures is manifested on the expression for the closest isotropic diffusion tensor; i.e. given a diffusion tensor, different tensor distance measures give rise to different closest isotropic tensor except for the Riemannian and Log-Euclidean distance measures which give the same closest isotropic tensor. Our experiments show that while FA shows better contrast between tissue classes within white matter, SA discriminates better between white matter and gray matter tissue classes. We demonstrate qualitatively that our new anisotropy measure reveals superior white matter profile of DT-MR brain images and analytically show that it has a higher signal to noise ratio than FA.

The paper is organized as follows: We first briefly review previous works in section 2 by presenting the mathematical development of FA in section 2.1 followed by the recently proposed tensor distance measures in section 2.2. Computation of closest isotropic tensor using the J-divergence and Log-Euclidean tensor distances is developed in section 2.3. Our new anisotropy measure is presented in section 3 and qualitatively compared with FA in section 4.1. The tissue discrimination power and signal to noise ratio of our new anisotropy measure is compared to FA in section 4.2 and section 4.3 respectively. Section 5 concludes the paper.

2. PREVIOUS WORK

2.1 Fractional Anisotropy Measure

The development of FA was first presented by Basser P.J. and Pierpaoli C..[1] Given diffusion tensor D, the authors propose decomposing D as

$$\begin{aligned} D &= D_{iso} + D_{an} \quad \text{with} && (1)\\ D_{iso} &= \bar{\lambda}\, I \quad \text{and} && (2)\\ D_{an} &= D - \bar{\lambda}\, I && (3) \end{aligned}$$

where $\bar{\lambda}$ is the mean of the eigenvalues of D and I is a 3×3 identity matrix. Clearly D_{iso} is isotropic tensor as it has equal eigenvalues $\lambda_1 = \lambda_2 = \lambda_3 = \bar{\lambda}$. D_{iso} is commonly referred to as the closest isotropic tensor to D. Having decomposed the diffusion tensor into its isotropic and anisotropic parts, the authors obtained scalar measures of their respective magnitudes (or lengths) by taking generalized tensor product as follows:

$$\|D_{iso}\| = \sqrt{\bar{\lambda}I : \bar{\lambda}I} = \bar{\lambda}\sqrt{I : I} = \sqrt{3}\bar{\lambda} \quad (4)$$

$$\|D\| = \sqrt{\sum_{i=1}^{3}\sum_{j=1}^{3} D_{i,j}^2} = \sqrt{\lambda_1^2 + \lambda_2^2 + \lambda_3^2} \quad (5)$$

$$\|D_{an}\| = \sqrt{\sum_{i=1}^{3}\sum_{j=1}^{3} (D_{i,j} - \bar{\lambda}I_{i,j})^2} = \sqrt{(\lambda_1 - \bar{\lambda})^2 + (\lambda_2 - \bar{\lambda})^2 + (\lambda_3 - \bar{\lambda})^2} \quad (6)$$

FA is then then defined as:

$$FA = \sqrt{\frac{3}{2}}\,\frac{\|D_{an}\|}{\|D\|} = \sqrt{\frac{3}{2}}\,\frac{\sqrt{(\lambda_1 - \bar{\lambda})^2 + (\lambda_2 - \bar{\lambda})^2 + (\lambda_3 - \bar{\lambda})^2}}{\sqrt{\lambda_1^2 + \lambda_2^2 + \lambda_3^2}} \quad (7)$$

It is clear that FA has range [0, 1] and it is rotationally invariant, scale invariant and sorting independent.[12] Moreover it has been demonstrated that FA map has a higher signal-to-noise ratio (SNR) than other anisotropy

measures such as relative anisotropy (RA) for any value of anisotropy greater than zero.[13] Note also that $\bar{\lambda}$ is chosen so that it minimizes the distance between D and D_{iso}, which can be solved by setting $D_{iso} = xI$ and then minimizing the distance $\|D - D_{iso}\| = \sqrt{(\lambda_1 - x)^2 + (\lambda_2 - x)^2 + (\lambda_3 - x)^2}$ to get $x = \frac{\lambda_1+\lambda_2+\lambda_3}{3}$.

2.2 Tensor Distance Measures

We consider two tensor distance metrics: The J-divergence distance measure(d_{JD})[7] and the Log-Euclidean distance metric (d_{LE})[8] given by:

$$d_{JD}(D_1, D_2) = \frac{1}{2}\sqrt{tr(D_1^{-1}D_2 + D_2^{-1}D_1) - 6} \quad (8)$$

$$d_{LE}(D_1, D_2) = \|log(D_1) - log(D_2)\|_2 \quad (9)$$

where tr denotes the trace of a matrix. Our aim is now to employ these distance metrics in order to compute the distance of a given diffusion tensor from its closest isotropic tensor.

Denoting the eigenvectors matrix of D as V and its diagonal matrix of eigenvalues as $\Lambda = diag(\lambda_1, \lambda_2, \lambda_3)$ and applying spectral decomposition, we obtain $D = V\Lambda V^T$, where T stands for matrix transposition. Noting that the closest isotropic tensor D_{iso} has the same set of eigenvectors as D (see details in Basser P.J. and Pierpaoli C.[1]) and denoting its eigenvalues matrix as $\bar{\Lambda} = diag(\bar{\lambda}, \bar{\lambda}, \bar{\lambda})$, we obtain $D_{iso} = V\bar{\Lambda}V^T$. Recalling that $VV^T = V^TV = I$, $D^{-1} = V\Lambda^{-1}V^T$, $log(D) = Vlog(\Lambda)V^T$, $\|D\|_2 = \sqrt{tr(D^TD)}$, and $tr(D) = tr(V\Lambda V^T) = tr(\Lambda) = \lambda_1 + \lambda_2 + \lambda_3$, it then easy to show that

$$\begin{aligned} d_{JD}(D, D_{iso}) &= \frac{1}{2}\sqrt{tr(D^{-1}D_{iso} + D_{iso}^{-1}D) - 6} \\ &= \frac{1}{2}\sqrt{tr(V\Lambda^{-1}\bar{\Lambda}V^T + V\bar{\Lambda}^{-1}\Lambda V^T) - 6} \\ &= \frac{1}{2}\sqrt{\sum_{i=1}^{3}\frac{\bar{\lambda}}{\lambda_i} + \sum_{i=1}^{3}\frac{\lambda_i}{\bar{\lambda}} - 6} \\ &= \frac{1}{2}\sqrt{\sum_{i=1}^{3}\frac{(\lambda_i - \bar{\lambda})^2}{\lambda_i\bar{\lambda}}} \end{aligned} \quad (10)$$

Similarly,

$$\begin{aligned} d_{LE}(D, D_{iso}) &= \|log(D) - log(D_{iso})\|_2 \\ &= \|V(log(\Lambda) - log(\bar{\Lambda}))V^T\|_2 \\ &= \|Vlog(\Lambda\bar{\Lambda}^{-1})V^T\|_2 \\ &= \sqrt{tr[Vlog^2(\Lambda\bar{\Lambda}^{-1})V^T]} \\ &= \sqrt{\sum_{i=1}^{3} log^2\Big(\frac{\lambda_i}{\bar{\lambda}}\Big)} \end{aligned} \quad (11)$$

Before proposing our anisotropy measure, let us first determine the closest isotropy to a given diffusion tensor for a given tensor distance measure.

2.3 Closest Isotropic Tensor

For the J-divergence distance measure, we start with Eq. 10 and set $\bar{\lambda}$ to an unknown variable x so that to minimize the function

$$f(x) = d_{JD}(D, xI) = \frac{1}{2}\sqrt{\sum_{i=1}^{3} \frac{(\lambda_i - x)^2}{\lambda_i x}} \tag{12}$$

Noting that minimizing f is same as minimizing f^2 because f is a non-negative function, we can find the value of x that minimizes f by differentiating f^2 with respect to x and setting the derivative to zero. After some calculations, we find that f takes minimum when

$$x = \sqrt{\frac{tr(D)}{tr(D^{-1})}} \tag{13}$$

Similarly, using the Log-Euclidean distance measure we minimize

$$f(x) = d_{LE}(D, xI) = \sqrt{\sum_{i=1}^{3} log^2\Big(\frac{\lambda_i}{x}\Big)} \tag{14}$$

to find *

$$x = \sqrt[3]{det(D)} \tag{15}$$

3. SHAPE ANISOTROPY INDEX (SA)

We make the following observations about Eqs. 10 and 11. Just like FA they are functions of eigenvalues only, they measure the distance of a tensor from its closest isotropy, and as D and D_{iso} differ only in shape but not orientation what these equations actually measure is the tensor shape distance between D and D_{iso}. However, unlike FA Eqs. 10 and 11 have range [0, $+\infty$). Therefore in order to derive anisotropy measure using these equations, we need to scale their range to [0, 1). Although there are several ways to achieve this, in this work we do this by taking the hyperbolic tangent of the distance of D from its closest isotropy as follows:

$$SA_{JD} = tanh\left(\sqrt{\sum_{i=1}^{3} \frac{(\lambda_i - \bar{\lambda})^2}{\lambda_i \bar{\lambda}}}\right) \tag{16}$$

$$SA_{LE} = tanh\left(\sqrt{\sum_{i=1}^{3} log^2\Big(\frac{\lambda_i}{\bar{\lambda}}\Big)}\right) \tag{17}$$

where $\bar{\lambda}$ is as shown in Eqs. 13 and 15. Since Eqs. 16 and 17 measure tensor shape distance scaled to the range [0, 1), we refer to these anisotropy measures as *Shape Anisotropy Index (SA)*. It is easy to see that SA, just like FA, is rotationally invariant, scale invariant, sorting of eigenvalues independent and has range [0, 1].

*Interestingly, the closest isotropy obtained in Eq. 15 using Log-Euclidean distance is the same closest isotropy obtained using the Riemannian tensor distance as shown in Batchelor et al.[10]

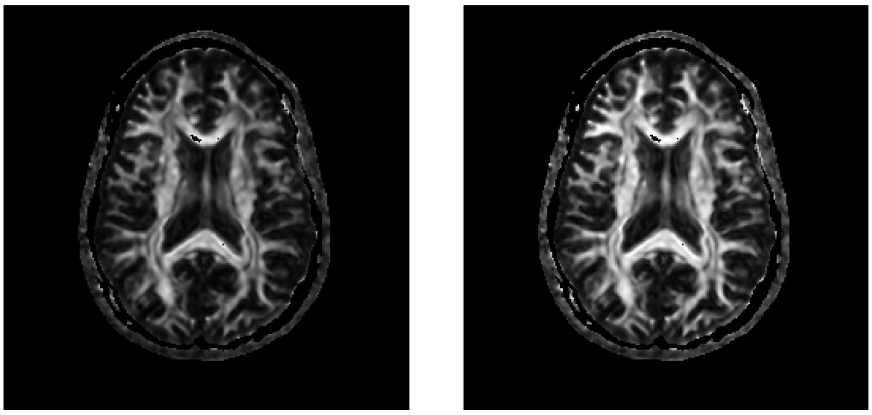

(a) FA (b) SA

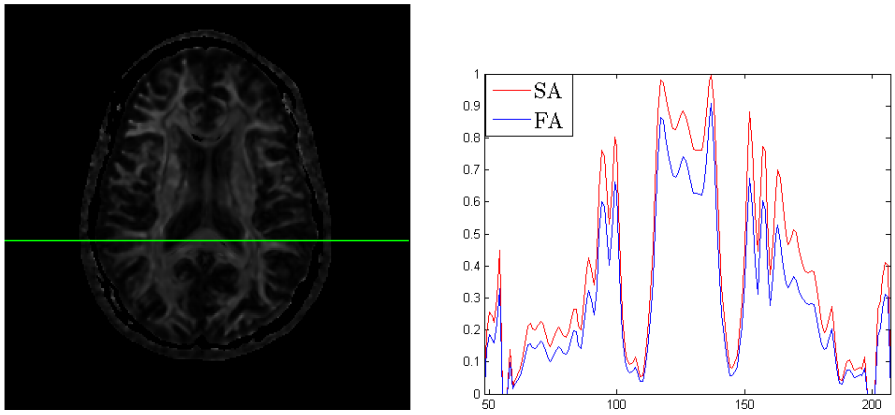

(c) SA minus FA (d) FA and SA profiles along the green line

Figure 1. Qualitative comparison of FA and SA maps using DT-MR brain image slice.

4. APPLICATIONS AND RESULTS

4.1 Qualitative Comparison of FA and SA

Qualitative comparison of FA and SA maps is shown in Fig. 1 using a real brain DT-MR image slice. Here we show only the result obtained using SA_{JD} because the result obtained using SA_{LE} is very similar. The diffusion weighted images were acquired using a Philips Achieva 3.0 Tesla scanner using 32 directions with slices parallel to the anterior commissure-posterior commissure line. 60 continuous slices of 2.2 mm thickness were collected with a field of view (FOV) of 212 mm, pixel size 0.8281 mm^2. We see from Figs. 1(a) and 1(b) that the SA map is brighter than FA which can also be seen in Fig. 1(c) where we show the difference between SA and FA maps (i.e. $SA - FA$). The intensity values of SA and FA maps are inspected along the green line shown in Fig. 1(c) and plotted in Fig. 1(d) which clearly shows SA map has higher intensity values than FA map along the line.

4.2 Tissue discrimination with FA and SA

Since SA takes consistently larger values than FA, we expect SA maps to provide better contrast between white matter and gray matter in the brain. This is demonstrated in Table 1 and Fig. 2 by first manually segmenting a slice of brain image to several different tissue classes and then calculating tissue detectability using FA and SA maps between pairs of tissue classes. For a pair of regions of interest ROI_1 and ROI_2 in an image whose mean and standard deviation intensity values are given respectively by $(< A_1 >, \sigma_1)$ and $(< A_2 >, \sigma_2)$, the tissue detectability for a given map (such as FA or SA) is calculated as[14]

$$d = \frac{< A_1 > - < A_2 >}{\sqrt{\sigma_1^2 - \sigma_2^2}} \tag{18}$$

Larger values of d between a pair of ROIs using a given map indicates that the map can better discriminate between the ROIs. The values of d shown in bold face indicate that the anisotropy index given on that row performs best in discriminating tissue classes given on the corresponding column. We observe that while FA performs better in detecting differences among tissues within the white matter; SA detects differences between white matter and gray matter regions better.

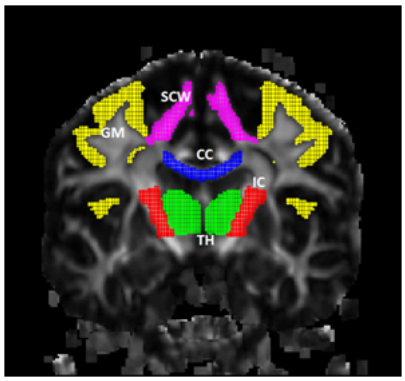

Figure 2. Single slice of FA map with corresponding regions of interest segmented: CC = corpus callosum, IC = Internal Capsule, TH = Thalamus, GM = Gray matter, and SCW = Subcortical white matter

Table 1. Tissue detectability using FA and SA

AI\ ROI	CC vs IC	CC vs TH	CC vs GM	CC vs SCW	IC vs TH	IC vs GM	IC vs SCW	TH vs GM	TH vs SCW	GM vs SCW
FA	0.24	**0.95**	2.01	**0.52**	**1.46**	2.69	**0.86**	2.07	**0.45**	1.82
SA_{JD}	**0.39**	0.74	**2.12**	0.36	1.35	**2.89**	0.81	2.10	0.36	**1.90**
SA_{LE}	0.38	0.73	2.10	0.37	1.33	2.87	0.82	**2.11**	0.34	1.89

4.3 Noise Immunity Considerations

While Fig. 1 gives a qualitative comparison of FA and SA maps, we now analytically show that SA has higher noise immunity than FA by comparing the signal to noise (SNR) of SA and FA. Once again, because the results obtained with SA_{JD} and SA_{LE} are very similar, here we report only the results obtained using SA_{JD}.

For any Anisotropy Index (AI) such as FA and SA; assuming that all λ_i's are independent with the same standard deviation (s.d.) of noise, the SNR of AI per unit s.d. of noise in λ_i is given by[13]

$$SNR(AI) = \frac{AI}{\sqrt{\sum_{i=1}^{3} \left(\frac{\partial AI}{\partial \lambda_i}\right)^2}} \tag{19}$$

Following the approach of Papadakis et al.,[13] we have calculated the values of AI and SNR of AI for FA and SA for a prolate tensor whose mean diffusivity $\bar{\lambda} = (\lambda_1 + \lambda_2 + \lambda_3)/3$ is kept constant at $0.7 \cdot 10^{-3} mm^2/s$, in agreement with typical values of the experimentally measured value for normal cerebral tissue. We then vary λ_1 from $0.7 \cdot 10^{-3} mm^2/s$ to $2.1 \cdot 10^{-3} mm^2/s$ and keep $\lambda_2 = \lambda_3 = (3\bar{\lambda} - \lambda_1)/2$. Fig. 3(a) shows plots of AI as a function of the dominant principal diffusivity λ_1 that was normalized relative to the mean diffusivity $\bar{\lambda}$. Fig. 3(a) shows that SA is consistently greater than or equal to FA which, as shown in[13] (c.f. fig 1(a)) and reproduced here, is greater than or equal to RA for all anisotropy levels. The gap between SA and FA is pronounced more

clearly as we move away from isotropic case and decreases as we approach the case of linear anisotropy. RA shows strongest linear variation with λ_1 than both FA and SA while SA depicts strongest non-linear variation.

Figure 3(b) shows plots of SNR(AI) as a function of the normalized dominant principal diffusivity λ_1. For small anisotropy levels, all RA, FA and SA have comparably same SNR but their differences in noise sensitivity becomes more prominent as anisotropy level increases with SA having better SNR than FA, which has higher SNR than RA (c.f. fig 1(b) in [13]). Therefore the SA maps will generally be more robust to noise than the FA and RA maps, exhibiting little intensity variation within structures of uniform anisotropy. The differences in the appearance of noise in the maps of the three AI's is more pronounced for the strongly anisotropic structures. Also note that SNR(SA) exceeds the axes limits for λ_1 values exceeding 2.5 (i.e. SA values exceeding 0.98).

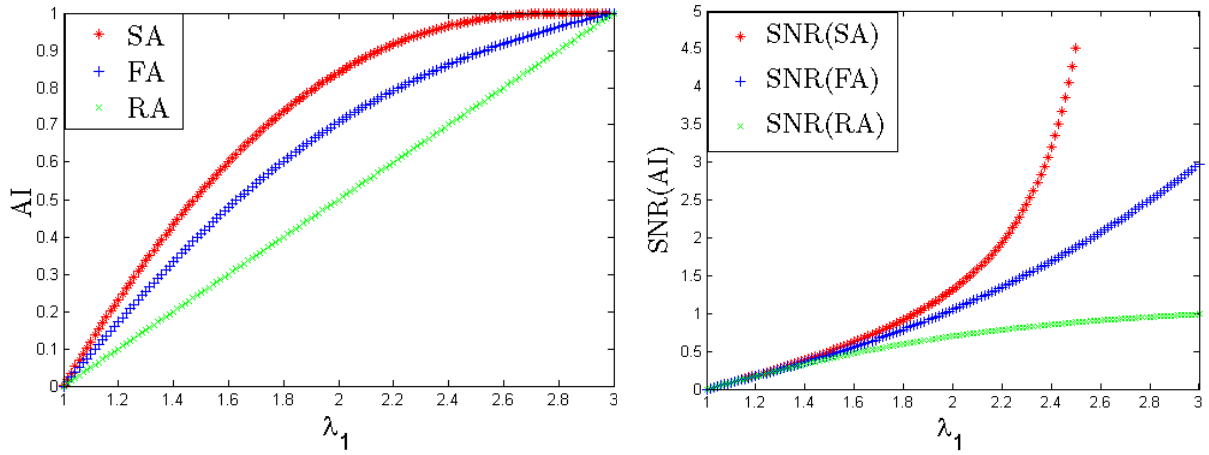

(a) RA, FA and SA of prolate tensor

(b) SNR of RA, FA and SA

Figure 3. AI and SNR(AI) of prolate tensor as its anisotropy varies from 0 to 1 as a function of the dominant principal diffusivity λ_1.

5. CONCLUSION

A novel anisotropy measure for DT-MRI is derived using tensor distance measures and its performance compared with existing anisotropy measures. Future work includes more validation of the proposed anisotropy measure and and its clinical use for the diagnosis and assessment of degenerative brain diseases as well as its application in the study of brain development. It remains to be seen if our method can be extended to higher order diffusion tensors such as fourth order tensors and to the newly emerging imaging techniques of Q-ball imaging in HARDI.

REFERENCES

[1] Basser, P. and Pierpaoli, C., "Microstructural and physiological features of tissues elucidated by quantitative-diffusion-tensor mri," *Magnetic Resonance, Series B* **111**(3), 209–219 (1996).

[2] Basser, P., "Fiber-tractography via diffusion tensor mri (dt-mri)," *Proceedings of the 6th Annual Meeting ISMRM, Sydney, Australia* **1226** (1998).

[3] Droogan, A., Clark, C., Werring, D., Barker, G., McDonald, W., and Miller, D., "Comparison of multiple sclerosis clinical subgroups using navigated spin echo diffusion-weighted imaging," *Magnetic Resonance Imaging* **17**(5), 653–661 (1999).

[4] Yoshikawa, K., Nakata, Y., Yamada, K., and Nakagawa, M., "Early pathological changes in the parkinsonian brain demonstrated by diffusion tensor mri," *British Medical Journal* **75**(3), 481–484 (2004).

[5] Lim, K., Hedehus, M., Moseley, M., de Crespigny, A., Sullivan, E., and Pfefferbaum, A., "Compromised white matter tract integrity in schizophrenia inferred from diffusion tensor imaging," *Archives of General Psychiatry* **56**(4), 367 (1999).

[6] Bozzali, M., Falini, A., Franceschi, M., Cercignani, M., Zuffi, M., Scotti, G., Comi, G., and Filippi, M., "White matter damage in alzheimer's disease assessed in vivo using diffusion tensor magnetic resonance imaging," *British Medical Journal* **72**(6), 742–746 (2002).

[7] Wang, Z. and Vemuri, B., "Dti segmentation using an information theoretic tensor dissimilarity measure," *IEEE Transactions on Medical Imaging* **24**(10), 1267–1277 (2005).

[8] Arsigny, V., Fillard, P., Pennec, X., and Ayache, N., "Log-euclidean metrics for fast and simple calculus on diffusion tensors," *Magnetic Resonance in Medicine* **56**(2), 411–421 (2006).

[9] Bhatia, R., [*Positive definite matrices*], Princeton University Press (2007).

[10] Batchelor, P., Moakher, M., Atkinson, D., Calamante, F., and Connelly, A., "A rigorous framework for diffusion tensor calculus," *Magnetic Resonance in Medicine* **53**(1), 221–225 (2005).

[11] Weldeselassie, Y. T., Hamarneh, G., Beg, M. F., and Atkins, M. S., "Novel decomposition of tensor distance into shape and orientation distances," *Medical Image Computing and Computer-Assisted Intervention Workshop on Diffusion Modelling and the Fibre Cup (MICCAI DMFC)* , 173–180 (2009).

[12] Westin, C., Maier, S., Mamata, H., Nabavi, A., Jolesz, F., and Kikinis, R., "Processing and visualization for diffusion tensor mri," *Medical Image Analysis* **6**(2), 93–108 (2002).

[13] Papadakis, N., Xing, D., Houston, G., Smith, J., Smith, M., James, M., Parsons, A., Huang, C., Hall, L., and Carpenter, T., "A study of rotationally invariant and symmetric indices of diffusion anisotropy," *Magnetic Resonance Imaging* **17**(6), 881–892 (1999).

[14] Alexander, A., Hasan, K., Kindlmann, G., Parker, D., and Tsuruda, J., "A geometric analysis of diffusion tensor measurements of the human brain," *Magnetic Resonance in Medicine* **44**(2), 283–291 (2000).